Journal of Rehabilitation in Civil Engineering 9-4 (2021) 62-76

journal homepage: http://civiljournal.semnan.ac.ir/

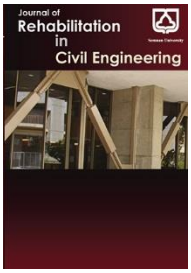

Correlation between Pulse-Like Ground Motion Intensity Measures and Seismic Demands of Buildings with Three Structural Systems (Moment-Resisting Frames, Structural Walls and Combination of Moment-Resisting Frames and Shear Walls)

Bakhtiyar Ghanbari[1], Mojtaba Fathi[1*]

1. Department of Civil Engineering, Razi University, Kermanshah, Iran
Corresponding author: *fathim@razi.ac.ir*

ARTICLE INFO

Article history:
Received: 25 November 2020
Revised: 28 January 2021
Accepted: 01 May 2021

Keywords:
Interstory drift ratio;
Continuum building model;
Pulse-like ground motions;
Lateral resisting system.

ABSTRACT

In this study, the distribution of correlation coefficients between maximum interstory drift ratio (MIDR) of multistorey building structures and ground motion characteristics intensity measures (IMs) is evaluated and compared. For this purpose, a continuum beam model is used to estimate the MIDR of multistory building structure including higher mode effects. The MIDRs are computed for building structures with three different lateral resisting systems (structural walls, moment-resisting frames, and their combination) and fundamental periods that ranges from 0.05 to 10s. Nine different ground motion parameters of pulse-like ground motions including PGD, PGA, PGV, Ic, CAV, Ia, SMV, ESD, SMA are selected as ground motion characteristics IMs. The effects of the type of lateral resisting system and the acceleration pulse on the distribution of correlation coefficients are also considered in the study. Based on the assessment results, MIDRs in mid and long-period buildings show a high correlation to PGV, SED and SMV, while a low correlation occurs with respect to PGA and SMA. Also, type of lateral resisting system causes changes in the correlation coefficients and results showed that long-period shear wall structure gives lower coefficients with respect to other structural systems.

1. Introduction

Selection of appropriate ground motion record for nonlinear dynamic analysis is a key challenge due to their notable effect on the interpretation of analysis outcomes. A common method for initial refinement of ground motion records with a minimum computational cost is application of refining process using an optimum intensity measure

How to cite this article:
Ghanbari, B., Fathi, M. (2021). Correlation between Pulse-Like Ground Motion Intensity Measures and Seismic Demands of Buildings with Three Structural Systems (Moment-Resisting Frames, Structural Walls and Combination of Moment-Resisting Frames and Shear Walls). Journal of Rehabilitation in Civil Engineering, 9(4), 62-76. https://doi.org/10.22075/JRCE.2021.21934.1458

(IM). The IM is key parameter in performance-based earthquake engineering framework which is able to quantitatively describe the critical characteristics of ground motion records [1, 2].

The available IMs can be categorized as two categories, i.e., structure-specific IMs and ground motion characteristics IMs. The ground motion characteristics IMs are only based on inherent information of ground motions and calculated directly from acceleration, velocity and displacement time histories of ground motion. Therefore, ground motion characteristics IMs can be categorized as three categories: velocity-related, acceleration-related, and displacement-related IMs. Peak Ground Velocity (PGV), Peak Ground Acceleration (PGA), peak Ground Displacement (PGD), Arias Intensity (Ia), Cumulative Absolute Velocity (CAV), and Specific Energy Density (SED) are recognized as ground motion IMs. The results of many studies indicate that correlation of PGV is higher than PGA [3-5]. The Ia is an important parameter for characterizing of energy of ground motions. The influence of Ia on the seismic response of structures has been studied by many researchers [6-7]. Mollaioli et al. [8] showed that for the base-isolated buildings the most efficient IMs are PGV and SED. Alvanitopoulos et al. [9] suggested two ground motion IMs to characterize the earthquake damage potential in structures. Pinzón et al. [10] suggested an ground motion IM based on the PGV.

More recently, characteristic peak ground acceleration have been proposed by Ganbari and Akhaveissy [11] to reduce the dispersion of Incremental dynamic analysis curves.

The structural damage measure (DM) characterizes the seismic response and damage to structures [12]. The DMs like maximum roof drift ratio (MRDR), maximum inter-story drift ratio (MIDR), and maximum floor acceleration (MFA) are widely used to develop structures and the structural damage. More recently, Mirrashid and Naderpour [13] and presented a computational model that represents the damage state of stories with consideration of damages in structural elements as well as the drift for damage state estimation of Reinforced Concrete (RC) frames under earthquake motions.

The maximum inter-story drift ratio (MIDR), refers to the highest values of the peak inter-story drift ratio of all stories above the ground. MIDR is a commonly utilized engineering demand parameter to assess damages to structures. For this purpose, a generalized interstory drift spectrum was developed by Miranda and Akkar [14] using a continuous combined model, where a shear beam and a flexural beam are coupled using rigid links. The simplified model was used to many studies to estimate maximum inter-story drift and floor acceleration demands in the structures subjected to pulse-like ground motions with velocity pulse and non-pulse motions. Khaloo and Khosravi [15] and Yang et al. [16] used the flexural-shear beam model to estimate maximum inter-story drift demands in buildings subjected to pulse-like ground motions with velocity pulse and non-pulse motions. Sahraei and behnamfar [17] developed a powerful type of nonlinear static analysis based on the continuum model called drift pushover analysis (DPA).

Alonso-Rodríguez and Miranda [18] investigated inter-storey drift and floor acceleration demand in buildings subjected to

near-fault ground motions by considering the simplified building and ground motion models. Neam and Taghikhany [19] used the continuum beam model to developed ground motion prediction equations for the estimation of generalized maximum interstory drift spectrum (GIDS) for three different common lateral resisting systems. Ghanbari and Akhaveissy [20] conducted a study to evaluate the influence of the pulse-like ground motion parameters on the inter-story drift ratio of buildings by using simple model. In another study, the seismic inter-story drift of high-rise buildings was estimated by the simple model [21]. The results of study show that the simple model provides an adequate estimation without the need for modelling and lengthy software analysis. Recently, an investigation was performed on the estimation of acceleration demands in building structures by means of dimensional analysis principles and low-order continuum models with a view to assessing the fragility of non-structural contents in structures behaving linearly or at the verge of yielding [22]. Zhang et al. [23] used the continuous beam model to develop a spectral-acceleration-based ground motion IM for high-rise buildings. A simplified frames (modified fish-bone model) was used by Soleimani et al. [24] to estimate nonlinear response of reinforced concrete frames subjected to earthquake excitation. Results of the above mentioned studies have shown that continuum building models have been successfully applied to describe the seismic response of multistorey building structures under pulse-like ground motion records. Pulse-like ground motions are very important due to their severe destructive effects on structures. The forward directivity effect, which includes a large velocity pulse at the beginning of the velocity time history of the ground motion, is the most damaging phenomenon observed in near-field pulse-like ground motions. Yahyaabadi and Tehranizadeh [25] developed scalar IMs (which use the root-mean-square of the spectral responses) to predict the seismic response of five 2D frame structures under pulse-like ground motions. Javadi and Yakhchalian [26] suggested PGV as optimal IM to characterize the near-fault ground motion damage potential in steel buckling restrained braced frames. D´avalos and Miranda [27, 28] introduced a ground motion IM, referred to as *FIV3*, for collapse estimation of moment-resisting frame buildings under ordinary and pulse-like ground motion records. Very recently, Zengin and Abrahamson [29, 30] developed a vector-valued IM that combines *S*a with instantaneous power (IP(T1)) to estimate the structural collapse under pulse-like ground motions. Recently, Palanci and Senel [31] used SDOF systems instead of multistory building to investigate the relation between ground motion IMS and DMS under ground motion records. There many studies reporting that the effect of higher modes can be specifically important for tall structures with long fundamental periods under near-fault pulse-like ground motions. The SDOF system neglects the influence of higher modes, so continuum building model is applied to estimate maximum inter-story drift of multistory building including higher mode effects in this study.

Main objective of this article is to investigate the relation between maximum inter-story drift ratio (MIDR) as a common engineering demand parameter and the ground motion characteristics IMs. For this purpose, continuum building models are utilized to measure the MIDR of multistory buildings and higher mode effects in particular. The

maximum inter-story drift ratio (MIDR) demands of the building structures obtained by using linear time history analyses under two sets pulse-like ground motion records (acceleration pulse and non-acceleration pulse). In this study, the effect of the type of acceleration pulse and lateral resisting systems are also regarded. Three structural systems with shear lateral deformation (moment-resisting frames), bending lateral deformation (shear walls), and hybrid lateral deformation (combination of moment-resisting frames and shear walls) are chosen.

2. Simplified model of a building structure

Simplified models are categorized into equivalent SDOF models and equivalent (MDOF) models. In recent decades, seismic response of structures was studied through examining structure response with SDOF system. The SDOF model does not represent local deformation of structure directly so that despite the simplicity, they are not accurate. Thus, simplified MDOF models have the accuracy to compute local deformation of structure, reduce the cost of computations, and are also suitable for linear and nonlinear time history analysis. In this study, a simplified continuous model is used to approximate the interstory drift of multistory buildings (Fig. 1). It consists of flexural and shear beams connected laterally by an infinite number of pin-jointed axially-rigid members. The dynamic response of un-damped continuous model is defined based on Equation 1 [14, 32]:

$$\frac{\rho}{EI}\frac{\partial^2 u(x,t)}{\partial t^2}+\frac{1}{H^2}\frac{\partial^4 u(x,t)}{\partial t^4}-\frac{\alpha^2}{H^4}\frac{\partial^2 u(x,t)}{\partial x^2}=-\frac{\rho}{EI}\frac{\partial^2 u_g(t)}{\partial t^2} \quad (1)$$

where ρ and H are the mass per unit length and the height of the continuous model, respectively. $u(x,t)$ denotes the lateral displacement of the model at the dimensionless height $x=z/H$ and time t. EI is the flexural stiffness of the flexural beam. α is the lateral stiffness ratio which is written as Equation 2 [13, 30]:

$$\alpha = H\sqrt{\frac{GA}{EI}} \quad (2)$$

in which GA indicate shear stiffness of the shear beam. $\alpha = 0$ and $\alpha = \infty$ corresponds to a pure flexural model and a pure shear model, respectively. The values of α are between 0 and 2 corresponds to a Structural wall building; the values of α for the buildings with dual structural systems consisting of a combination of moment-resisting frames and shear walls or a combination of moment-resisting frames and braced frames is typically between 1.5 and 6; for the moment-resisting frame buildings, α is between 5 and 20 [13, 30]. In Fig. 2, each kind of lateral resisting system is illustrated. The interstory drift ratio of buildings is key parameters to measure the damage of structural and nonstructural components and defined as the difference of displacements at the adjacent two floors normalized by the inter-story height. The inter-story drift ratio at the jth story of a building structure can be computed by the following equation [14, 32]:

$$IDR(j,t)\approx\theta(x,t)=\frac{1}{H}\sum_{i=1}^{\infty}\Gamma_i\phi_i'(x)D_i(t) \quad (3)$$

Where Γ_i is the modal participation factor of the ith mode of vibration of the continuous beam model that can be calculated by the following equation [14, 32]:

$$IDR(j,t)\approx\frac{1}{H}\sum_{i=1}^{m}\Gamma_i\phi_i'(x)D_i(t) \quad (4)$$

$\phi_i'(x)$ means the amplitude of the ith mode at non dimensional height x, $D_i(t)$ denotes the relative displacement response of a SDOF system corresponding to the ith mode. m is the number of vibration modes considered. The maximum interstory drift spectra (MIDR) is a plot of the natural vibration

period T of the building versus the maximum interstory drift ratio. For a given fundamental period, the total height of the model in Eq.(4) is calculated using the relationship suggested steel moment-resistant frame in the 1997 UBC code, namely, $T_1=0.0853H^{0.75}$ [14,32].

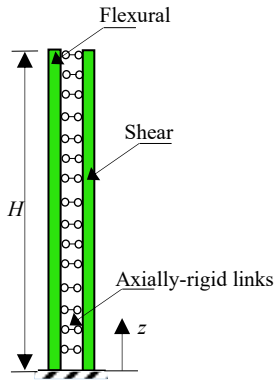

Fig 1. Simplified beam model of multi-story building (Miranda and akkar, 2006).

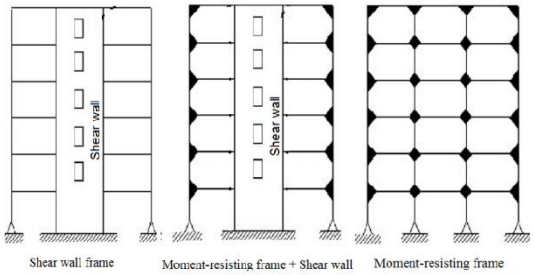

Fig 2. Schematic configuration of the three lateral resisting systems.

2. Ground motion intensity measures

To evaluation the influence of the high frequency component of pulse-like ground motion on the seismic response of structure, some researchers used decomposition methods in time domain to extract velocity pulse [33-37].Very recently, a new technique to extract velocity and acceleration pulse of forward directivity effects of new-field ground motions was introduced by Chang Z et al., [38, 39]. The technique uses wavelet transformation to decompose the original pulse-like ground motion, extract pulse period, and determine record as acceleration pulses and non-acceleration pulses.

This study utilizes a set of pulse-like ground motions that includes 41 acceleration pulses and 38 non-acceleration pulses from Chang Z et al. [39] (expressed in Appendix). Fig. 2 shows acceleration time histories of TCU052-E (RSN1492) record with distinct acceleration pulse and TCU076-E (RSN11511) record without acceleration pulse recorded during the 1999 Chi-Chi earthquake. For the 79 selected pulse-like ground motions, the distribution of PGV with regard to D_{rup} was analyzed, as shown in Fig. 3. In the assessment of the correlation between MIDR and ground motion characteristics IMs, 9 ground motion intensity measures are collected and listed in Table 1, where their definitions are presented in three groups, i.e. acceleration-related, velocity-related and displacement-related IMs.

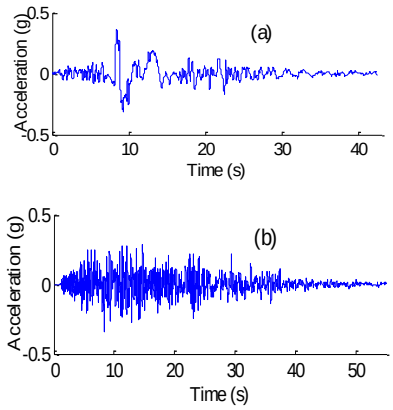

Fig 2. Acceleration time-histories of a) TCU052-E (RSN1492) record with visible pulse; b) TCU076-E (RSN11511) record without visible pulse from1999 Chi-Chi earthquake.

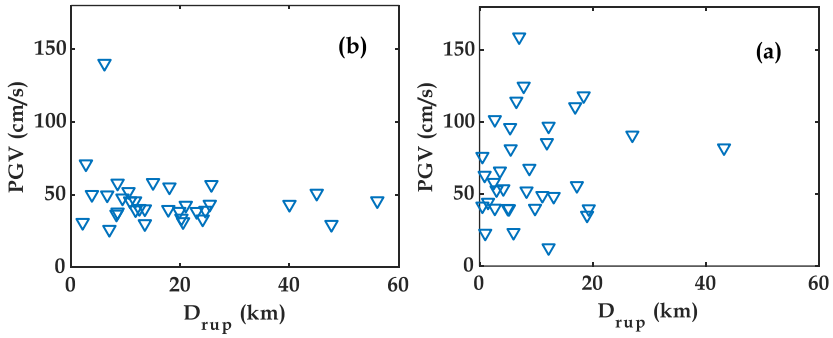

Fig 3. Distribution of PGV with distance to fault for a) acceleration pulse b) non-acceleration pulse records.

3. Structural damage measure (*DM*)

In this study, maximum interstory drift ratio (MIDR) was chosen as the structural damage measure (DM) due to its good correlation with the structural damage under strong pulse-like ground motions [40]. MIDR spectrum compute for eight vibration modes (m = 8) and three values of lateral stiffness ratios (α =0.01, 4 and 15) represent three kind of familiar lateral resisting systems under selected pulse-like ground motions. To introduce three different lateral resisting systems, α equaling 1 is chosen for structures with flexural deformation (such as shear wall structure), α equaling 15 represents structures under shear deformation (such as moment-resisting frame), and α represents four 4 corresponds to multistory buildings that contains both overall shear and flexural lateral deformations (e.g., hybrid moment frame + shear wall). In this study, the fundamental vibration period T of the building ranged from 0.05s to 10s with an incremental of 0.05 (i.e., 200 values of period) and viscous damping ratio ξ assumed 5%. Fig. ٤ describes the major steps to calculate MIDR of buildings under the pulse type ground motion.

The variation of MIDR rate versus fundamental period of building structure is displayed for multistory buildings with flexural (α=1) and shear (α=15) deformation systems under two typical pulse-like ground motions (acceleration pulse and non-acceleration pulse) in Fig. ٥. It is clear that the MIDR values increases in the short-to medium -period region and decreases in the ling period region. A comparison of these figures reveals that in medium- and long-period buildings (1 < T < 3.5 s), acceleration pulse motions induce larger interstory drift ratio demands and the MIDR demands for the acceleration pulse records can be twice as much as those induced by non- acceleration pulse records**.** It is noteworthy that the buildings with long periods (T > 3.5 s) are equivalently taken as base-isolated buildings.

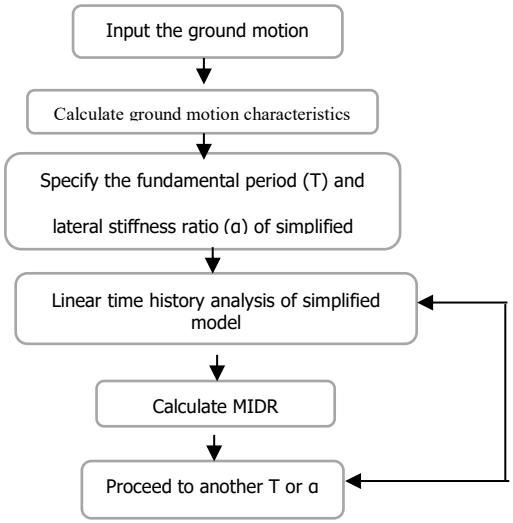

Fig. 4. Detail of analysis procedure to calculate the maximum interstory drift ratio, MIDR.

4. Correlation between ground motion IMs and maximum inter-story drift ratio (MIDR)

The Pearson correlation coefficient between two variables IM and DM, is given by the following relation:

$$p = \frac{n(\sum xy)-(\sum x)(\sum y)}{\sqrt{[n\sum x^2-(\sum x)2].[n\sum y^2-(\sum y)2]}} \quad (5)$$

where, x and y represent the ground motion intensity measure and maximum inter-story drift ratio demand under the pulse-like ground motion, respectively; n is the total number of selected pulse-like ground motions. The correlation coefficient p varies from -1.0 and 1.0. Closer absolute value of p to 1.0 denotes better IM-DM correlation.

Table 1. Selected ground motion intensity measures.

Intensity measure(IM)	Definition	References
Acceleration-related		
PGA= max$\lvert \ddot{ug}(t) \rvert$	Peak ground acceleration	N.A.
$I_A = \frac{\pi}{2g}\int_0^{T_f}[\ddot{ug}(t)]^2\,dt$	Arias intensity	(Arias, 1970) [41]
CAV =$\int_0^{T_f}\lvert \ddot{ug}(t) \rvert\,dt$	Cumulative absolute velocity	(Reed & Kassawara, 1990) [42]
$I_C = \sqrt{\frac{1}{t2-t1}\int_{t1}^{t2}[\ddot{ug}(t)]^2\,dt}$	Characteristic intensity	
SMA	Sustained maximum acceleration	(Nuttli, 1979)[43]
Velocity-related		
PGV=max$\lvert \dot{ug}(t) \rvert$	Peak ground velocity	N.A.
SED = $\int_0^{T_f}[\dot{ug}(t)]^2\,dt$	Specific energy density	N.A.
SMV	Sustained maximum velocity	(Nuttli, 1979)
Displacement-related		
PGD = max $\lvert ug(t) \rvert$	Peak ground displacement	N.A

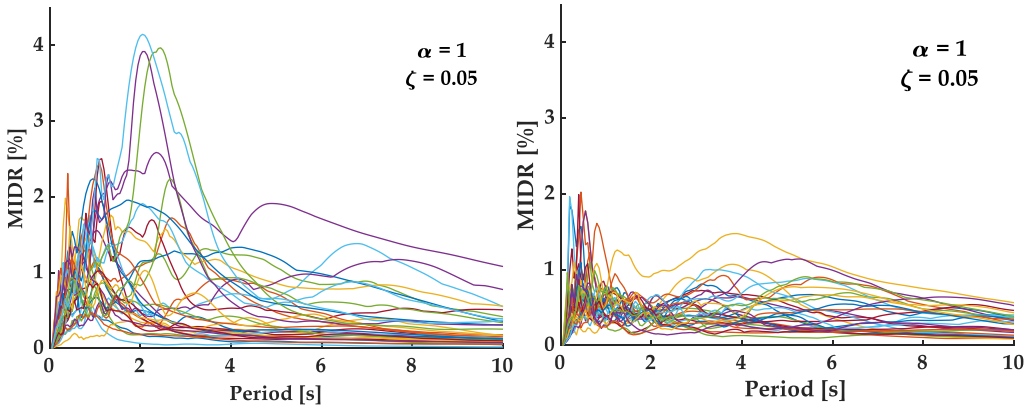

Fig. 5. MIDR spectrum for lateral stiffness ratio, α =0.01 (Left: acceleration pulses, Right: non-acceleration pulse records).

5. Results

Fig. ۶, illustrates the correlation values of selected ground motion IMs for the structural systems. Clearly, PGV, SED, and SMV are correlated with MIDRs in medium and long-period structures (T>2s). In addition, the structural system has a significant effect on PGV and SMV results in mid/long-period ranges. In the case of structures in this period (T>2s), PGA and SMA have a low correlation with the MIDRs. In addition, IMs CAV, SED, and SMV have a negative correlation with MIDRs in buildings of short period (T<0.5s) with different structural systems.

In addition, it can be seen in Figures 6 that the correlation coefficient of structural system of shear deformation system is too close to hybrid behavior system. The MIDRs of buildings with shear wall systems have a low correlation coefficient as to other structural systems in mid/long-period buildings (T>2s). Clearly, velocity-related IMs can predict the MIDR of all buildings with hybrid and shear lateral deformation behavior. As shown, the correlations of PGD have similar trends for all lateral resisting systems in every period range.

Fig. ۷, illustrates the correlation values of ground motion IMs for the acceleration and non-acceleration pulse records. The results of analyses indicate that the type of pulse-like ground motions affect the correlation coefficient of selected ground motion IMs. In the case of medium and long-period buildings structures, velocity related IMs (PGV, SMV, and SED) of acceleration pulse record have good correlation with the MIDRs.

Between short and medium period (0.1-1.5s) correlation coefficients of non-acceleration pulse records exceed the correlation of acceleration pulse records. Clearly, the results of IM CAV are significantly affected by acceleration pulse.

In addition, there is a strong correlation between the CAV parameter of non-acceleration pulse record and MIDRs of short-period buildings with shear lateral deformation system. The acceleration pulse of CAV has a good correlation with the MIDR of medium and long-period buildings. As the results indicate, the correlation trend of SED of acceleration and non-acceleration pulse record have a good similarity in medium/long-period structures subjected to pulse-like ground motions. In the case of acceleration pulse record, the negative correlation coefficients are obtained for IM SED of short-period buildings with shear lateral deformation system. There is a low correlation between IM Ia and MIDR demands of long-period buildings featured with bending lateral deformation (shear walls). This is true for the two types of pulse-like records.

In Fig. 8, calculations of correlation coefficient at 1 s and 4.0 s fundamental period building structures are displayed. Results show that MIDRs increase with decreasing lateral stiffness ratio and because of this situation positive correlation coefficient values are obtained.

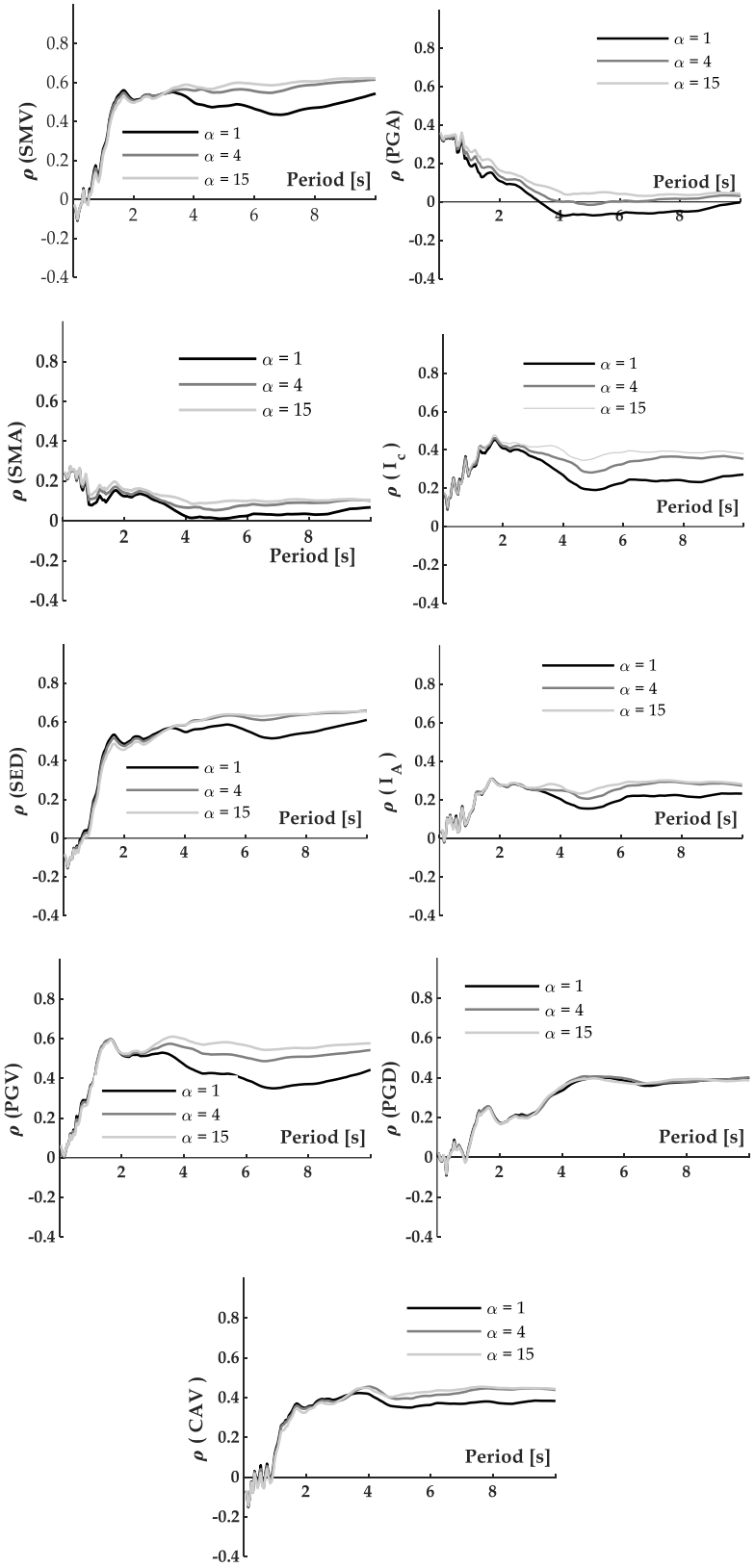

Fig. 6. Correlations between MIDR and ground motion IMs for three lateral stiffness ratios (α =0.01, 4 and 15).

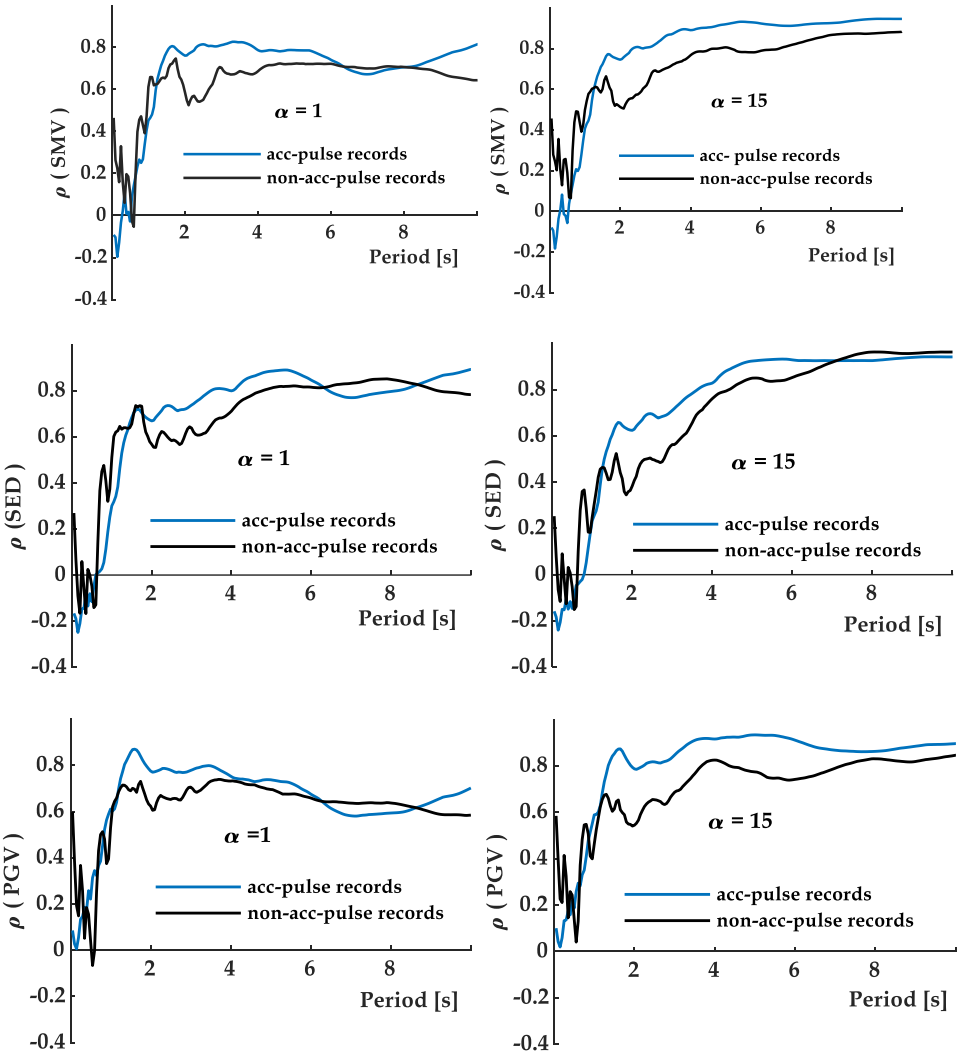
ρ (SMV)
α = 1
acc-pulse records
non-acc-pulse records
Period [s]
ρ (SMV)
α = 15
acc- pulse records
non-acc-pulse records
Period [s]
ρ (SED)
α = 1
acc-pulse records
non-acc-pulse records
Period [s]
ρ (SED)
α = 15
acc-pulse records
non-acc-pulse records
Period [s]
ρ (PGV)
α =1
acc-pulse records
non-acc-pulse records
Period [s]
ρ (PGV)
α = 15
acc-pulse records
non-acc-pulse records
Period [s]

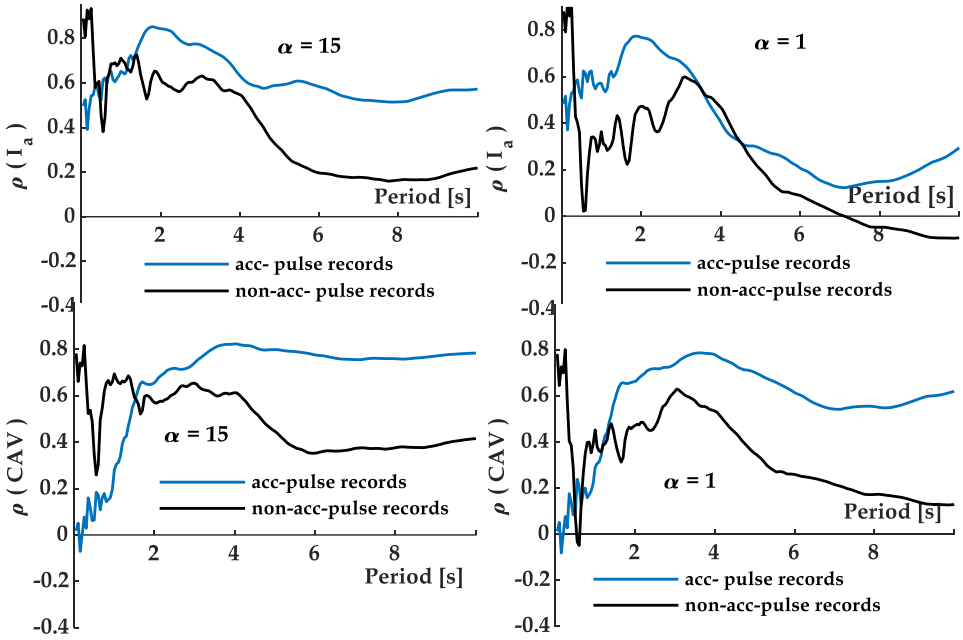

Fig. 7 Effect of acceleration pulse on the ground motion IMs correlations with MIDR.

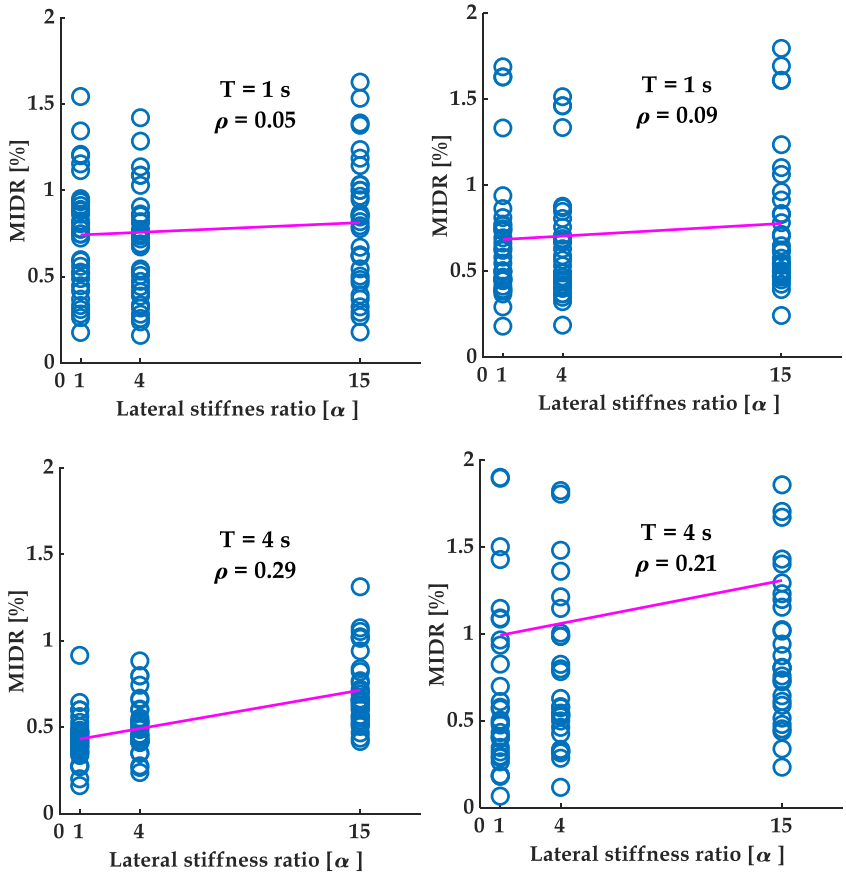

Fig. 8 Correlation of MIDRs demand and lateral stiffness ratios (α) (Left: acceleration pulses, Right: non-acceleration pulse records).

6. Summary and conclusions

This manuscript focused on the distribution of correlation coefficients of ground motion characteristics IMs and the maximum interstory drift ratio (MIDR) of multistorey building structures. For this purpose, a continuum building model was used to obtain MIDR of multistorey building structures. The effect of different lateral resisting systems on the correlations was considered. Three structural featuring shear lateral deformation (moment-resisting frames), bending lateral deformation (shear walls), and hybrid lateral deformation (combination of moment-resisting frames and shear walls) were selected. The correlation coefficients of Pearson between the pulse-like ground motion IMs and the MIDRs of building structures were calculated and comprehensive evaluation conducted in the present study show the following findings.

The strongest correlations were found for velocity-related IMs (PGV, SMV, and SED) that were highly correlated with MIDRs of mid/long-period building structures.

As shown by the results, the effect of lateral resisting systems grows with the periods of building structures. In the case of structures with medium/long-periods (T>2s), the correlation coefficients obtained by $\alpha = 1$ (such as shear wall building) are relatively lower than other structural systems.

In the case of acceleration pulse records, the SED and SMV IMs have a strong correlation with the MIDR of the building structure featured with a deformation of shear lateral (moment-resisting frames).

In general, the results are indicative of higher correlation coefficients of IMs of SED and SMV as to other ground motion IMs for mid/long-period structures. In addition, the sensitivity of the IM to the acceleration pulse can be moderated.

Eventually, it is notable that these observations and conclusions are for the linear response of building structures and nonlinear so that nonlinear seismic response is not included. There is a need for deeper examination of correlation coefficients between ground motion IMs and nonlinear seismic response of the simple models of multistorey structures.

7. Appendix

see Tables A1 and A2

Table A1. Presents the dataset of acc-pulse records used in the dynamic analyses.

No	Earthquake	Component	Year	*M*	*R* [km]	PGA g	V_{s30} m/s	T_P(s) by S_v	T_P(s) by PPM
1	Loma Prieta	LOMAP/A02043	1989	6.93	43.2	0.26	133	1.1	**1.1**
2	Loma Prieta	LOMAP/ GGB270	1989	6.93	79.8	0.22	584	1.2	**1.3**
3	Loma Prieta	LOMAP/ LEX000	1989	6.93	5.0	0.19	1070	1.1	**1**
4	Loma Prieta	LOMAP/ LEX090	1989	6.93	5.0	0.44	1070	1.2	**1.1**
5	Loma Prieta	LOMAP/G04360	1989	5.74	5.7	0.41	222	0.9	**1**
6	Loma Prieta	LOMAP/CYC195	1989	6.19	0.5	0.38	561	0.8	**0.7**
7	N.palm Springs	NPS210	1986	6.06	4	0.69	345	0.9	**1.2**
8	Whittier Narrows-01	A-OR2010	1987	5.99	24.5	0.35	345	0.8	**0.7**
9	Northridge-01	NORTHR/JGB022	1994	6.69	5.4	0.44	526	2.9	**2.9**
10	Northridge-01	NORTHR/WPI046	1994	6.69	5.5	0.57	286	1.8	**2**
11	Northridge-01	NORTHR/WPI316	1994	6.69	5.5	0.47	286	1.4	**2**
12	Northridge-01	NORTHR/SCE281	1994	6.69	5.2	0.42	371	1.3	**2.2**
13	Northridge-01	NORTHR/SYL090	1994	6.69	5.3	0.36	441	1.9	**2.4**
14	Cape Mendocino	NORTHR/CPM000	1994	7.01	7	0.42	568	2.4	**0.9**
15	Chi-Chi, Taiwan	CHICHI/ CHY006-W	1999	7.62	9.8	0.56	438	1.8	**1.9**
16	Chi-Chi, Taiwan	CHICHI/TCU018-N	1999	7.62	66.3	0.36	573	5.5	**7.3**

17	Chi-Chi, Taiwan	CHICHI/ TCU052-E	1999	7.62	0.7	0.13	579	5.7	**5.6**
18	Chi-Chi, Taiwan	CHICHI/ TCU063-N	1999	7.62	9.8	0.06	476	4	**3.6**
19	Chi-Chi, Taiwan	CHICHI/ TCU064-N	1999	7.62	16.6	0.12	646	5.2	**7.6**
20	Chi-Chi, Taiwan	CHICHI/ TCU067-E	1999	7.62	0.6	0.5	434	2.2	**2.3**
21	Chi-Chi, Taiwan	CHICHI/ TCU075-E	1999	7.62	0.9	0.33	573	3.9	**4.2**
22	Chi-Chi, Taiwan	CHICHI/ TCU087-N	1999	7.62	7	0.11	573	3.8	**4.5**
23	Chi-Chi, Taiwan	CHICHI/ TCU102-E	1999	7.62	1.5	0.3	714	2.9	**2.6**
24	Chi-Chi, Taiwan	CHICHI/ TCU128-E	1999	7.62	13.1	0.14	600	5.5	**7.4**
25	Chi-Chi, Taiwan	CHICHI/ TCU136-N	1999	7.62	8.3	0.17	462	3.4	**7.2**
26	Cape Mendocino	CAPE.M/ BNH360	1992	7.01	12.2	0.21	566	1.9	**2.2**
27	Cape Mendocino	CAPE.M/ FFS270	1992	7.01	19.3	0.38	388	1.4	**1.3**
28	Cape Mendocino	CAPE.M/ FFS360	1992	7.01	19.3	0.27	388	1.0	**1.4**
29	Bam, Iran	BAM-L	2003	6.6	1.7	0.81	487	1.5	**1.7**
30	Bam, Iran	BAM-T	2003	6.6	1.7	0.63	487	1.5	**1.4**
31	Parkfield	PARKFIELD/SCN360	2004	6	3.0	0.35	648	0.8	**0.7**
32	Parkfield	PARKFIELD/ C01090	2004	6	3.0	0.44	327	1.3	**1.2**
33	Parkfield	PARKFIELD/ C01360	2004	6	3.0	0.36	327	1.1	**0.8**
34	Parkfield	PARKFIELD/ C02090	2004	6	3.0	0.62	173	0.7	**0.9**
35	Parkfield	PARKFIELD/ C02360	2004	6	3.0	0.37	173	0.8	**0.7**
36	Parkfield	PARKFIELD/ C03360	2004	6	3.6	0.33	231	0.8	**0.9**
37	Parkfield	PARKFIELD/ C02360	2004	6	3.0	0.58	173	0.8	**0.7**
38	Parkfield	PARKFIELD/ Z14090	2004	6	8.8	0.58	246	0.7	**0.6**
39	Parkfield	PARKFIELD/ C04090	2004	6	4.2	0.51	410	0.6	**0.5**
40	Parkfield	PARKFIELD/ PRK360	2004	6	2.7	0.83	265	1.1	**1.2**
41	Parkfield,2004	PARKFIELD/ PRK360	2004	6	2.7	0.31	265	1.1	**1.2**

Table A2. Presents the dataset of non-acc-pulse records used in the dynamic analyses.

No	Earthquake	Component	Year	M	R [km]	PGA g	V_{s30} m/s	$T_P(s)$ by S_v	$T_P(s)$ by PPM
1	Tabas, Iran	TAB-T1	1989	7.35	2.1	0.85	767	5	**4.7**
2	Loma Prieta	LOMAP/ STG090	1989	6.93	8.5	0.32	381	3.5	**5.4**
3	Landers	LANDERS/ LCN260	1989	7.28	2.2	0.73	1369	5.1	**4.7**
4	Kocaeli, Turkey	KOCAELI/ ARE000	1989	7.51	13.5	0.21	523	4.6	**8.3**
5	Kocaeli, Turkey	KOCAELI/ ARE090	1989	7.51	13.5	0.12	523	4.1	**5.8**
6	Kocaeli, Turkey	KOCAELI/ IZT090	1989	7.51	7.2	0.23	811	3.9	**1.9**
7	Duzce, Turkey	DUZCE/DZC180	1999	7.14	6.6	0.4	345	3.8	**5.4**
8	Duzce, Turkey	DUZCE/487-NS	1999	7.13	2.7	0.3	690	5.2	**7.6**
9	Hector Mine	HECTOR/ HEC000	1994	6.61	5.9	0.27	446	3.7	**0.4**
10	Tottori, Japan	TOTT/ SMNH01EW	1994	6.52	6.2	0.27	411	2.4	**1.3**
11	San Simeon, CA	SAN/36695090	1994	6.52	6		371	1.6	**3.1**
12	Iwate/Japan	IWATE/IWTH26NS	1994	6.9	20.2	0.9	479	3.9	**3.7**
13	Iwate/Japan	IWATE/MYG004NS	1994	6.9	24.1	0.75	655	4	**4**
14	Iwate/Japan	IWATE/56362EW	1994	6.9	7	0.16	568	2.4	**5.6**
15	El Mayor-Cucapah	EI.M/CIWESHNN	1999	7.2	11.4	0.26	242	6.6	**5.2**
16	Chi-Chi, Taiwan	CHICHI/ TCU036-N	1999	7.62	19.8	0.12	478	6.3	**7.7**
17	Chi-Chi, Taiwan	CHICHI/ TCU038-N	1999	7.62	25.4	0.14	298	6.5	**10**
18	Chi-Chi, Taiwan	CHICHI/ TCU026-E	1999	7.62	56.1	0.16	570	6.8	**5.3**
19	Chi-Chi, Taiwan	CHICHI/ TCU040-E	1999	7.62	22.1	0.28	362	4.9	**10**
20	Chi-Chi, Taiwan	CHICHI/ TCU049-E	1999	7.62	3.8	0.15	487	6.3	**10**
21	Chi-Chi, Taiwan	CHICHI/ TCU050-E	1999	7.62	9.5	0.16	298	6.5	**8.5**
22	Chi-Chi, Taiwan	CHICHI/ TCU051-E	1999	7.62	7.6	0.23	570	5.5	**8.8**
23	Chi-Chi, Taiwan	CHICHI/ TCU053-E	1999	7.62	6	0.15	362	4.3	**8.1**
24	Chi-Chi, Taiwan	CHICHI/ TCU054-E	1999	7.62	5.3	0.16	542	6.1	**8.8**
25	Chi-Chi, Taiwan	CHICHI/ TCU056-E	1999	7.62	10.5	0.34	350	6.5	**3.7**
26	Chi-Chi, Taiwan	CHICHI/ TCU076-E	1999	7.62	2.7	0.23	455	3.2	**7.5**
27	Chi-Chi, Taiwan	CHICHI/ TCU082-E	1999	7.62	5.2	0.12	461	6.2	**8.4**
28	Chi-Chi, Taiwan	CHICHI/ TCU087-E	1999	7.62	7	0.53	403	5.3	**0.7**
29	Chi-Chi, Taiwan	CHICHI/ TCU088-N	1999	7.62	18.2	0.11	615	4.9	**7.2**
30	Chi-Chi, Taiwan	CHICHI/ TCU098-E	1999	7.62	47.7	0.11	473	8.2	**7.1**
31	Chi-Chi, Taiwan	CHICHI/ TCU100-E	1999	7.62	11.4	0.26	462	6.4	**5.1**
32	Chi-Chi, Taiwan	CHICHI/ TCU101-N	1999	7.62	2.1	0.1	389	4.4	**5.4**
33	Chi-Chi, Taiwan	CHICHI/ TCU104-E	1999	7.62	12.9	0.17	410	6.6	**5.4**
34	Chi-Chi, Taiwan	CHICHI/ TCU136-W	1999	7.62	8.3	0.4	462	6.9	**9.7**
35	El Mayor-Cucapah	EI MAY/CIWESHNN	2004	7.2	11.4	0.33	242	6.6	**5.6**
36	Darfield, New Zeland	DAFIELD/DSLCN27W	2004	7	8.5	0.26	296	6	**6.8**
37	Darfield, New Zeland	DAFIELD/DSLCN63E	2004	7	8.5	0.28	296	5.4	**6.4**
38	Darfield, New Zeland	DAFIELD/HVSCS26W	2004	7	24.5	0.58	422	3.4	**0.5**

REFERENCES

[1] Moehle, J., & Deierlein, G. G. (2004). "A framework methodology for performance-based earthquake engineering. Paper presented at Proceedings of the 13th World Conference on Earthquake Engineering (Paper No. 679). Vancouver, BC, Canada.

[2] Stewart, J. P., Chiou, S. J., Bray, J. D., Graves, R. W., Somerville, P. G., & Abrahamson, N. A. (2002). "Ground motion evaluation procedures for performance-based design." Soil Dynamics and Earthquake Engineering, 22(9-12), 765–772. https://doi.org/10.1016/S0267-7261(02)00097-0

[3] Kramer, S. L. [1996] "Geotechnical Earthquake Engineering, Prentice Hall, Englewood Cliffs.

[4] Ebrahimian, H., Jalayer, F., Lucchini, A., Mollaioli, F., & Manfredi, G. (2015). "Preliminary ranking of alternative scalar and vector intensity measures of ground shaking." Bulletin of Earthquake Engineering, 3(10), 2805–2840. https://doi.org/10.1007/s10518-015-9755-9

[5] Kohrangi, M, Bazzurro, P and Vamvatsikos, D (2016). "Vector and Scalar IMs in Structural Response Estimation, Part II: Building Demand Assessment." Earthquake Spectra 32(3), 1525-1543. https://doi.org/10.1193/053115EQS080M

[6] Kostinakis, K., Fontara, I. K., & Athanatopoulou, A. M. (2018). "Scalar structure-specific ground motion intensity measures for assessing the seismic performance of structures: A review." Journal of Earthquake Engineering, 22(4), 630–665.https://doi.org/10.1080/13632469.2016.1264323

[7] Hu, J., & Liu, H. (2019). "Identification of ground motion intensity measure and its application for predicting soil liquefaction potential based on the Bayesian network method. "Engineering Geology, 248, 34-49.https://doi.org/10.1016/j.enggeo.2018.11.006

[8] Mollaioli, F., Lucchini, A., Cheng, Y., & Monti, G. (2013). "Intensity measures for the seismic response prediction of base-isolated buildings. " Bulletin of Earthquake Engineering, 11(5), 1841-1866. https://doi.org/10.1007/s10518-013-9431-x

[9] Alvanitopoulos P F, Andreadis I and Elenas A2010Interdependence between damage indices and ground motion parameters based on Hilbert–Huang transform Meas. Sci. Technol. 21 025101.

[10] Pinzón, L. A., Vargas-Alzate, Y. F., Pujades, L. G., & Diaz, S. A. (2020). "A drift-correlated ground motion intensity measure: Application to steel frame buildings. " Soil Dynamics and Earthquake Engineering, 132, 106096. https://doi.org/10.1016/j.soildyn.2020.106096

[11] Ghanbari, B., & Akhaveissy, A. H. (2020). "Evaluation of characteristic peak ground acceleration (CPGA) as a ground motion intensity measure to reduce the dispersion of IDA curves." https://doi.org/10.1007/s42107-020-00259-7

[12] Riddell, R. (2007). "On ground motion intensity indices." Earthquake Spectra, 23(1), 147–173. https://doi.org/10.1193/1.2424748

[13] Mirrashid, M., & Naderpour, H. (2021). Innovative Computational Intelligence-Based Model for Vulnerability Assessment of RC Frames Subject to Seismic Sequence. Journal of Structural Engineering, 147(3), 04020350. DOI: 10.1061/(ASCE)ST.1943-541X.0002921.

[14] Miranda, E., & Akkar, S. D. (2006). "Generalized interstory drift spectrum. Journal of structural engineering, 132(6), 840-852. https://doi.org/10.1061/(ASCE)0733-9445(2006)132:6(840)

[15] Khaloo, A. R., & Khosravi, H. (2008). "Multi-mode response of shear and flexural buildings to pulse-type ground motions in near-field earthquakes." Journal of Earthquake Engineering, 12(4), 616-630. https://doi.org/10.1080/13632460701513132

[16] Yang, D., Pan, J., & Li, G. (2010). " Interstory drift ratio of building structures subjected to near-fault ground motions based on generalized drift spectral analysis. " Soil Dynamics and Earthquake Engineering, 30(11), 1182-1197. https://doi.org/10.1016/j.soildyn.2010.04.026

[17] Sahraei, A., & Behnamfar, F. (2014). "A drift pushover analysis procedure for estimating "the seismic demands of buildings. Earthquake Spectra, 30(4), 1601-1618. https://doi.org/10.1193/030811EQS038M

[18] Alonso-Rodríguez, A., & Miranda, E. (2015). "Assessment of building behavior under near-fault pulse-like ground motions through simplified models." Soil Dynamics and Earthquake Engineering, 79, 47-58. https://doi.org/10.1016/j.soildyn.2015.08.009

[19] Neam, A. S., & Taghikhany, T. (2016). "Prediction equations for generalized interstory drift spectrum considering near-fault ground motions." Natural Hazards, 80(3), 1443-1473. https://doi.org/10.1007/s11069-015-2029-7

[20] Ghanbari, B., & Akhaveissy, A. H. (2017). "Effects of pulse-like ground motions parameters on inter-story drift spectra of multi-story buildings." International Journal of Structural Engineering, 8(1), 60-73. 10.1504/IJSTRUCTE.2017.081671

[21] Ranaiefar, M. A., Hosseini, M. H., & Mansoori, M. R. (2019). Estimating Inter-Story Drift in High Rise Buildings with the Flexural and Shear Cantilever Beam and Mode-Acceleration Method. *Journal of Rehabilitation in Civil Engineering*, *7*(2), 164-177. https://10.22075/JRCE.2018.12200.1209

[22] Málaga-Chuquitaype, C., Psaltakis, M. E., Kampas, G., & Wu, J. (2019). "Dimensionless fragility analysis of seismic acceleration demands through low-order building models. " Bulletin of Earthquake Engineering, 17(7), 3815-3845. https://doi.org/10.1007/s10518-019-00615-2

[23] Zhang, Y., He, Z., Lu, W., & Yang, Y. (2018). "A spectral-acceleration-based linear combination-type earthquake intensity measure for high-rise buildings. " Journal of Earthquake Engineering, 22(8), 1479-1508. https://doi.org/10.1177/1369433219894237

[24] Soleimani, R., Khosravi, H., & Hamidi, H. (2019). Substitute Frame and adapted Fish-Bone model: Two simplified frames representative of RC moment resisting frames. *Engineering Structures*, *185*, 68-89.
https://doi.org/10.1016/j.engstruct.2019.01.127

[25] Yahyaabadi, A., & Tehranizadeh, M. (2012). "Development of an improved intensity measure in order to reduce the variability in seismic demands under near-fault ground motions. " Journal of Earthquake and Tsunami, 6(02), 1250012.
https://doi.org/10.1142/S1793431112500121

[26] Javadi, E., & Yakhchalian, M. (2019). "Selection of optimal intensity measure for seismic assessment of steel buckling restrained braced frames under near-fault ground motions." Journal of Rehabilitation in Civil Engineering, 7(4), 114-133. 10.22075/JRCE.2018.14908.1278

[27] Dávalos, H., Heresi, P., & Miranda, E. (2020). "A ground motion prediction equation for filtered incremental velocity, FIV3. Soil Dynamics and Earthquake Engineering, 139, 106346.
https://doi.org/10.1016/j.soildyn.2020.106346

[28] Dávalos, H., & Miranda, E. (2020). "Evaluation of FIV3 as an intensity measure for collapse estimation of moment-resisting frame buildings." Journal of Structural Engineering, 146(10), 04020204.
https://doi.org/10.1061/(ASCE)ST.1943541X.0002781

[29] Zengin, E., & Abrahamson, N. A. (2020). "A vector-valued intensity measure for near-fault ground motions." Earthquake Engineering & Structural Dynamics, 49(7), 716-734.
https://doi.org/10.1016/j.engstruct.2007.07.009

[30] Zengin, E., & Abrahamson, N. (2020). "Conditional Ground-Motion Model for Damaging Characteristics of Near-Fault Ground Motions Based on Instantaneous Power." Bulletin of the Seismological Society of America, 110(6), 2828-2842.
https://doi.org/10.1785/0120200124

[31] Palanci, M., & Senel, S. M. (2019). "Correlation of earthquake intensity measures and spectral displacement demands in building type structures."Soil Dynamics and Earthquake Engineering, 121, 306-326.
https://doi.org/10.1016/j.soildyn.2019.03.023

[32] Miranda, E., & Taghavi, S. (2005). "Approximate floor acceleration demands in multistory buildings. I: Formulation. Journal of structural engineering, 131(2), 203-211.https://doi.org/10.1061/(ASCE)0733 9445(2005)131:2(203)

[33] Baker, J. W. (2007). Quantitative classification of near-fault ground motions using wavelet analysis. *Bulletin of the Seismological Society of America*, *97*(5), 1486-1501.

[34] Zhao, G. C., Xu, L., & Xie, L. (2016). Study on low-frequency characterizations of pulse-type ground motions through multi-resolution analysis. *Journal of Earthquake Engineering*, *20*(6), 1011-1033.
https://doi.org/10.1080/13632469.2015.1104761

[35] Zhao, G., Xu, L., Gardoni, P., & Xie, L. (2019). A new method of deriving the acceleration and displacement design spectra of pulse-like ground motions based on the wavelet multi-resolution analysis. *Soil Dynamics and Earthquake Engineering*, *119*, 1-10.
https://doi.org/10.1016/j.soildyn.2019.01.008

[36] Yalcin, O. F., & Dicleli, M. (2020). Effect of the high frequency components of near-fault ground motions on the response of linear and nonlinear SDOF systems: a moving average filtering approach. *Soil Dynamics and Earthquake Engineering*, *129*, 105922.
https://doi.org/10.1016/j.soildyn.2019.105922

[37] Chen, X., & Wang, D. (2020). Multi-pulse characteristics of near-fault ground motions. *Soil Dynamics and Earthquake Engineering*, *137*, 106275.
https://doi.org/10.1016/j.soildyn.2020.106275

[38] Chang, Z., De Luca, F., & Goda, K. (2019). "Near-fault acceleration pulses and non-acceleration pulses: Effects on the inelastic displacement ratio." Earthquake Engineering & Structural Dynamics, 48(11), 1256-1276.
https://doi.org/10.1002/eqe.3184

[39] Chang, Z., De Luca, F., & Goda, K. (2019). Automated classification of near-fault acceleration pulses using wavelet packets. Computer-Aided Civil and Infrastructure Engineering, 34(7), 569-585.
https://doi.org/10.1111/mice.12437

[40] Razi, M., Vahdani, R., Gerami, M., & Farrokhshahi, F. (2019). "Seismic Fragility Assessment of Steel SMRF Structures under Various Types of Near and Far Fault Ground Motions." Journal of Rehabilitation in Civil Engineering, 7(2), 86-100.
10.22075/JRCE.2018.11039.1179

[41] Arias A (1970). "A measure of earthquake intensity. In: Hansen R (ed) Seismic design for nuclear power plants. MIT Press, Cambridge.

[42] Reed, J. W., & Kassawara, R. P. (1990). A criterion for determining exceedance of the operating basis earthquake. Nuclear Engineering and Design, 123(2-3), 387–396. doi:10.1016/0029-5493(90)90259-Z.
https://doi.org/10.1016/0029-5493(90)90259-Z

[43] Nuttli OW (1979) The relation of sustained maximum ground acceleration and velocity to earthquake intensity and magnitude. US Army Engineer Waterways Experiment Station, Vicksburg.